RESEARCH ARTICLE OPEN ACCESS

Carbon Nanotubes On Unsteady MHD Non-Darcy Flow Over A Porous Wedge In The Presence Of Thermal Radiation Energy

R. Kandasamy, Radiah Mohammad , I. Muhaimin
Research Centre For Computational Mathematics, Fstpi,
Universiti Tun Hussein Onn Malaysia, Malaysia

ABSTRACT
Thermal radiation energy technologies are clean sources of energy that have a much lower environmental impact than conventional energy technologies. The objective of the present work is to investigate theoretically the effect of copper nanoparticles and carbon nanotubes in the presence of base fluid (water) with variable stream condition due to thermal radiation energy. Single wall carbon nanotubes (SWCNTs) in the presence of base fluid flow over a porous wedge plays a significant role compared to that of copper nanoparticles on absorbs the incident solar radiation and transmits it to the working fluid by convection.
Keywords: Carbon nanotubes; Copper nanoparticles; Magnetic field; Thermal radiation energy

I. INTRODUCTION

Thermal radiation energy is receiving more and more attention as governments are trying to shift from fossil fuel-based energy sources to more natural and renewable options. Nanofluids – engineered colloidal suspensions of nanoparticles in a base fluid – are attracting a great deal of interest with their enormous potential to provide enhanced performance properties. Particularly with respect to heat transfer, and compared with more conventional heat transfer fluids (i.e. coolants) currently available, nanofluidic coolants exhibit enhanced thermal conductivity. Attempts to increase the thermal conductivity of heat transfer fluidsusing nanoparticles have been an active research area over the past decade. The researchers, led by Lalwani et al. [1], Nield and Kuznetsov[2], Kuznetsov and Nield [3] and Khan and Pop [4] found that their single-walled carbon nanotube (SWCNT) nanofluid exhibits an increase in conductivity of up to almost (15-20)%; a value significantly higher than what has been achieved with nanoparticle-based nanofluids. Single walled carbon nanotubes (SWCNT) have unique electronic and mechanical properties which can be used in numerous applications, such as field-emission displays, nanocomposite materials, nanosensors, and logic elements.
Feng-Chao Wang and Ya-Pu Zhao [5]investigated that the slip boundary conditions based on kinetic theory and molecular dynamic simulations.
^ This paper was recommended for publication in revised form by Associate Editor 000 000

The results predicted that the momentum transfer among the liquid layers and the bulk liquid must be considered according to the wetting conditions of the solid surface, which can interpret the contradictory published results of slip behavior at high shear stress. In the case of SWCNTs, covalent functionalization will break some carbon double bonds, leaving "holes" in the structure of the nanotube and, thus, modifying both its mechanical and electrical properties, Treacy et al [6]. Retraction force that occurs in telescopic motion caused by the Lennard-Jones interaction between shells and its value is about 1.5 nN, Zavalniuk and Marchenko [7].
Quanzi Yuan and Ya-Pu Zhao [8,9] studied that the transport properties of confined water in a SWCNT are different from bulk water in view of configuration, the diffusion coefficient, the dipole orientation, and the density distribution.

A voltage difference of several millivolts could generate between the two ends of a SWCNT due to interactions between the water dipole chains and charge carriers in the tube. Hence, the structure of a water-filled SWCNT can be a dominant candidate for a synthetic nanoscale power cell as well as a practical nanopower harvesting device.

Based on the aforementioned, it could be stated that little published literature exists regarding SWCNTs in water and their applications as heat transfer fluid. Also, there is inconsistency in the few reported studies on the convective heat behavior of CNT-nanofluids. Therefore, it was decided to study the convective heat transfer behavior of SWCNTs in water in laminar flow regimes.

II. MATHEMATICAL ANALYSIS

Let us consider an unsteady laminar two-dimensional non-Darcy flow of an incompressibleviscous nanofluid past a porous

wedge in the presence of solar energy radiation. The fluid is a water based nanofluid containing copper nanoparticles and single walled carbon nanotubes. The working fluid is assumed to have heat absorption properties and the porous medium absorbs the incident thermal radiation energy and transmits it to the working fluid by convection. The thermophysical properties of the nanofluids are given in Tables 1-3. Under the same assumptions of Kandasamy et al. [10], the boundary layer equations governing the flow and thermal field are defined as

$$\frac{\partial \bar{u}}{\partial \bar{x}} + \frac{\partial \bar{v}}{\partial \bar{y}} = 0 \tag{1}$$

$$\frac{\partial \bar{u}}{\partial \bar{t}} + \bar{u}\frac{\partial \bar{u}}{\partial \bar{x}} + \bar{v}\frac{\partial \bar{u}}{\partial \bar{y}} = \frac{1}{\rho_{f_n}}\left[\frac{\partial U}{\partial t}\rho_{f_n} + U\frac{dU}{dx}\rho_{f_n} + \mu_{f_n}\frac{\partial^2 \bar{u}}{\partial \bar{y}^2} + (\rho\beta)_{f_n}\bar{g}(T - T_\infty)\sin\frac{\Omega}{2} - \frac{F}{\sqrt{K}}\rho_{f_n}(\bar{u}^2 - U^2) - (\sigma B_0^2 + \frac{\nu_f}{K}\rho_{f_n})(\bar{u} - U)\right] \tag{2}$$

$$\frac{\partial T}{\partial \bar{t}} + \bar{u}\frac{\partial T}{\partial \bar{x}} + \bar{v}\frac{\partial T}{\partial \bar{y}} = \alpha_{f_n}\frac{\partial^2 T}{\partial \bar{y}^2} - \frac{1}{(\rho c_p)_{f_n}}\frac{\partial q''_{rad}}{\partial y} + \frac{\mu_{f_n}}{(\rho c_p)_{f_n}}\left(\frac{\partial u}{\partial y}\right)^2 \tag{3}$$

where $q''_{rad} = -\frac{4\sigma_1}{3k^*}\frac{\partial T^4}{\partial y}$ (Sparrow and Cess [11]), σ_1 - the Stefan–Boltzman constant is, k^* - the mean absorption coefficient. The boundary conditions of these equations are

$$\bar{u} = 0, \bar{v} = -v_0, T = T_w + c_1 x^{n_1} \text{ at } \bar{y} = 0;$$

$$\bar{u} \to U = \frac{\nu_f x^m}{\delta^{m+1}}, T \to T_\infty \text{ as } \bar{y} \to \infty \tag{4}$$

c_1 *and* n_1 (power index) - constants, v_0 - the suction (> 0) or injection (< 0) velocity, T_w - the fluid temperature at the plate, $U(x,t) = \frac{\nu_f x^m}{\delta^{m+1}}$ - the potential flow velocity, $\beta_1 = \frac{2m}{1+m}$ - the angle of the wedge, $\delta = \delta(t)$ - the time-dependent length scale, $\beta_1 = \frac{\Omega}{\pi}$ - a total angle Ω of the wedge, w and ∞ - surface and ambient conditions, $\bar{u}$ and $\bar{v}$ - the velocity components in the $\bar{x}$ and $\bar{y}$ directions, T - the local temperature of the nanofluid, $\bar{g}$ - the acceleration due to gravity, K - the permeability of the porous medium, F - the empirical constant in the second-order resistance, K - the permeability of the porous medium, ρ_{nf} - the effective density of the nanofluid, μ_{nf} - the effective dynamic viscosity of the nanofluid and α_{nf} - the thermal diffusivity of the nanofluid.

$$\rho_{nf} = (1-\varphi)\rho_f + \varphi\rho_{CNT}, \mu_{nf} = \frac{\mu_f}{(1-\varphi)^{2.5}},$$

$$\alpha_{nf} = \frac{k_{nf}}{(\rho c_p)_{nf}},$$

$$(\rho c_p)_{nf} = (1-\varphi)(\rho c_p)_f + \varphi(\rho c_p)_{CNT},$$

$$\frac{k_{nf}}{k_f} = \left\{\frac{(k_{CNT} + 2k_f) - 2\varphi(k_f - k_{CNT})}{(k_{CNT} + 2k_f) + 2\varphi(k_f - k_{CNT})}\right\} \tag{5}$$

In the limit of low particle volume concentration (φ) and the nanoparticle conductivity (k_s), being much higher than the base liquid conductivity (k_f). μ_f - the viscosity of base fluid, φ - the nanoparticle fraction, $(\rho c_p)_{nf}$ - the effective heat capacity of a CNT, k_{nf} - the thermal conductivity of nanofluid, k_f and k_{CNT} - the thermal conductivities of the base fluid and CNT and ρ_f and ρ_{CNT} - the thermal conductivities of the base fluid and CNT. Following the lines of Kafoussias and Nanousis [13], the changes of variables are

$$\eta = y\sqrt{\frac{(1+m)}{2}}\sqrt{\frac{x^{m-1}}{\delta^{m+1}}}, \psi = \sqrt{\frac{2}{1+m}}\frac{\nu_f x^{\frac{m+1}{2}}}{\delta^{\frac{m+1}{2}}} f(\eta) \text{ and } \theta = \frac{T - T_\infty}{T_w - T_\infty} \tag{6}$$

The stream function ψ is defined as $u = \frac{\partial \psi}{\partial y}$ and $v = -\frac{\partial \psi}{\partial x}$, the system of the symmetry groups of Equs. (2) and (3) are calculated using the classical Lie group approach (Kandasamy et al. [14]). Equations (2) and (3) become

$$f''' - \frac{\frac{2}{m+1}(1-\zeta)^{2.5}\xi^2}{(1-\zeta+\zeta\frac{\rho_s}{\rho_f})}\left[(M + \frac{\lambda}{(1-\zeta)^{2.5}})(f'-1) - \xi^{\frac{1}{1-m}}\{(1-\zeta+\zeta\frac{(\rho c_p)_s}{(\rho c_p)_f})\}\gamma\sin\frac{\Omega}{2}\theta\right] - (1-\zeta+\zeta\frac{\rho_s}{\rho_f})$$

$$(1-\zeta)^{2.5}\left[\frac{2}{m+1}(m - F_n)(f'^2 - 1) - f f'' + \lambda_u(2 - \eta f'' - 2f') + \frac{1-m}{1=m}\xi\frac{\partial f}{\partial \xi}\left(\frac{\partial f}{\partial \eta} - \frac{\partial^2 f}{\partial \eta^2}\right)\right] = 0 \tag{7}$$

$$\theta'' + \frac{4}{3}\frac{k_f}{k_{f_n}} N\{(C_T+\theta)^3\theta'\}' + \frac{\Pr_f}{(1-\zeta)^{2.5}} Ec\,(f'')^2$$
$$- \Pr_f\{1-\zeta+\zeta\frac{(\rho c_p)_s}{(\rho c_p)_f}\}\frac{k_f}{k_{f_n}}[\frac{2n_1}{m+1} f'\theta - f\theta'$$
$$+ \lambda_\upsilon \eta\,\theta' + \frac{1-m}{1+m}\{\xi\frac{\partial\theta}{\partial\xi}\frac{\partial f}{\partial\eta} - \xi\frac{\partial f}{\partial\xi}\frac{\partial\theta}{\partial\eta}\}] = 0 \quad (8)$$

The boundary conditions take the following form

$$\frac{\partial f}{\partial\eta} = 0, \frac{m+1}{2} f + \frac{1-m}{2}\xi\frac{\partial f}{\partial\xi} = -S, \theta = 1 \text{ at } \eta = 0$$
$$\text{and } \frac{\partial f}{\partial\eta} = 1, \theta \to 0 \text{ as } \eta \to \infty \quad (9)$$

$\Pr_f = \frac{\nu_f}{\alpha_f}$ - Prandtl number, $\lambda = \frac{\nu_f x}{KU}$ - the porous media parameter, $\gamma = \frac{Gr}{\mathrm{Re}^2}$ - the buoyancy or natural convection parameter, $Gr = \frac{g(\beta)_f \Delta T x^3}{\nu_f^2}$ - the Grashof number, $\mathrm{Re} = \frac{U x}{\nu_f}$ - the Reynolds number, $N = \frac{4\sigma_1\theta_w^3}{k_f k^*}$ - the conductive radiation parameter, $F_n = \frac{Fx}{\sqrt{K}}$ - Forchheimer number, $Ec = \frac{U^2}{(c_p)_f (T_w - T_\infty)}$ - the Eckert number, $M = \frac{\sigma B_0^2 x}{U\rho_f}$ - the magnetic parameter, where $x = \left(\frac{\xi}{k}\right)^{\frac{2}{1-m}}$ and $C_T = \frac{T_\infty}{T_w - T_\infty}$ is the temperature ratio and C_T assumes very small values by its definition as $T_w - T_\infty$ is very large compared to T_∞. In the present study, $C_T = 0.1$. It is mentioning that $\gamma > 0$ aids the flow and $\gamma < 0$ opposes the flow, while $\gamma = 0$ i.e., $(T_w - T_\infty)$ represents the case of forced convection flow. On the other hand, if γ is of a significantly greater order of magnitude than one, then the buoyancy forces will be predominant. Hence, combined convective flow exists when $\gamma = O(1)$. S - the suction parameter if $S > 0$ and injection if $S < 0$ and $\xi = k\,x^{\frac{1-m}{2}}$ Kafoussias and Nanousis [13], at the first level of truncation, the terms accompanied by $\xi\frac{\partial}{\partial\xi}$ are small. This is particularly true when (ξ <<1). Thus the terms with $\xi\frac{\partial}{\partial\xi}$ on the right-hand sides of Equations (7) and (8) are deleted to get the following system of equations:

$$f''' - \frac{\frac{2}{m+1}(1-\zeta)^{2.5}\xi^2}{(1-\zeta+\zeta\frac{\rho_s}{\rho_f})}[(M + \frac{\lambda}{(1-\zeta)^{2.5}})(f'-1) - \xi^{\frac{1}{1-m}}$$
$$\{(1-\zeta+\zeta\frac{(\rho c_p)_s}{(\rho c_p)_f})\}\gamma\sin\frac{\Omega}{2}\theta] - (1-\zeta+\zeta\frac{\rho_s}{\rho_f})(1-\zeta)^{2.5}[\frac{2}{m+1}$$
$$(m - F_n)(f'^2 - 1) - f f'' + \lambda_u(2 - \eta f'' - 2f')] = 0 \quad (10)$$

$$\theta'' + \frac{4}{3}\frac{k_f}{k_{f_n}} N\{(C_T+\theta)^3\theta'\}' + \frac{\Pr_f}{(1-\zeta)^{2.5}} Ec\,(f'')^2$$
$$- \Pr_f\{1-\zeta+\zeta\frac{(\rho c_p)_s}{(\rho c_p)_f}\}$$
$$\frac{k_f}{k_{f_n}}[\frac{2n_1}{m+1} f'\theta - f\theta' + \lambda_\upsilon\eta\,\theta'] = 0 \quad (11)$$

The boundary conditions take the following form

$$f' = 0, f = -\frac{2S}{m+1}, \theta = 1 \text{ at } \eta = 0 \text{ and}$$
$$f' = 1, \theta \to 0 \text{ as } \eta \to \infty \quad (12)$$

Further, $\lambda_\upsilon = \frac{c}{x^{m-1}}$ where $c = \frac{\delta^m}{\nu_f}\frac{d\delta}{dt}$ and integrating, $\delta = [c(m+1)\nu_f t]^{\frac{1}{m+1}}$. When $c = 2$ and $m = 1$ in δ and we get $\delta = 2\sqrt{\nu_f t}$ which shows that the parameter δ can be compared with the well established scaling parameter for the unsteady boundary layer problems (see Schlichting [15]).

For practical purposes, the skin friction coefficient and the Nusselt number are defined as

$$C_f = \frac{\mu_{f_n}}{\rho_f U^2}\left(\frac{\partial u}{\partial y}\right)_{at\ y=0} = -\frac{1}{(1-\zeta)^{2.5}}(\mathrm{Re}\ x)^{-\frac{1}{2}} f''(0)$$
$$Nu_x = \frac{xk_{f_n}}{k_f(T_w - T_\infty)}\left(\frac{\partial T}{\partial y}\right)_{at\ y=0} =$$
$$-(\mathrm{Re}\ x)^{\frac{1}{2}}\frac{k_{f_n}}{k_f}\theta'(0)\left[1 + \frac{4}{3}N(C_T + \theta(0))^3\right] \quad (13)$$

Here, $\mathrm{Re}_x = \frac{U x}{\nu_f}$ is the local Reynolds number.

III. RESULTS AND DISCUSSION

The system of equations (10) and (11) are highly nonlinear coupled equations and cannot be solved analytically and numerical solutions subject to the boundary conditions (12) are obtained using the very robust computer algebra software Maple 18. This software uses a fourth-fifth order Runge–Kutta–Fehlberg method with shooting technique as default to solve the boundary value problems numerically using the dsolve command. For the benefit of the readers the Maple worksheet is listed in Appendix A. The numerical results are represented in the form of the dimensionless velocity and temperature in the presence of SWCNT and copper nanoparticles.

Table 1 Important features of carbon nanotubes

Carbon nanotubes	purit %	Outer diameter [nm]	Inner diameter [nm]	Length [μm]	Specific surface [m^2 /g]
MWCNTs	>95	8-15	3-5	10-50	233
SWCNTs	>90	1-2	0.8-1.6	5-30	407

Table 2 Thermophysical properties of fluid and nanoparticles

	$\rho(kg/m^3)$	$c_p(J/kgK)$	$k(W/mK)$	$\beta\times10^{-5}(K^{-1})$
Pure water	997.1	4179	0.613	21
Copper (Cu)	8933	385	401	1.67
Silver (Ag)	10500	235	429	1.89
Alumina (Al_2O_3)	3970	765	40	0.85
Titanium (TiO_2)	4250	6862	8.9538	0.9
SWCNTs	2600	425	6600	27
MWCNTs	1600	796	3000	44

Table 3 Thermophysical properties of different base fluids and CNTs

Physical properties	Base fluid		
	Water	Ethylene glycol	Engine oil
$\rho(kg/m^3)$	997	1115	884
$c_p(J/kg\ K)$	4179	2430	1910
$k(W/m\ K)$	0.613	0.253	0.144
Pr	6.2	203.63	6450

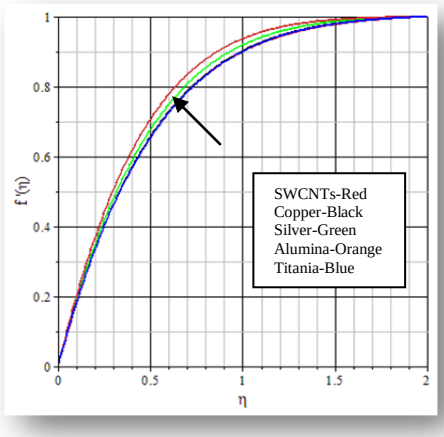

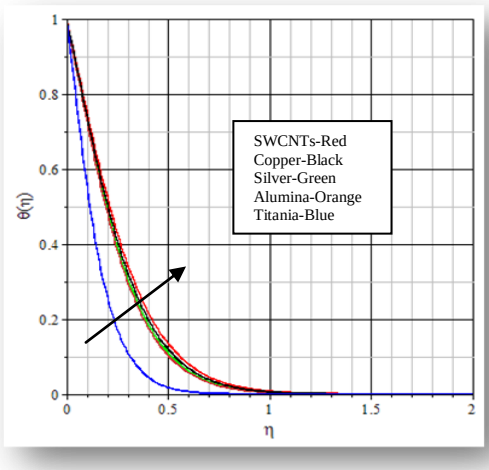

Fig.1 Effects of water based SWCNTs and nanoparticles on velocity and temperature profiles

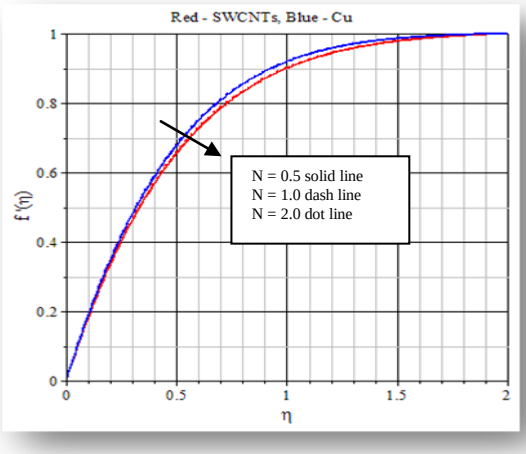

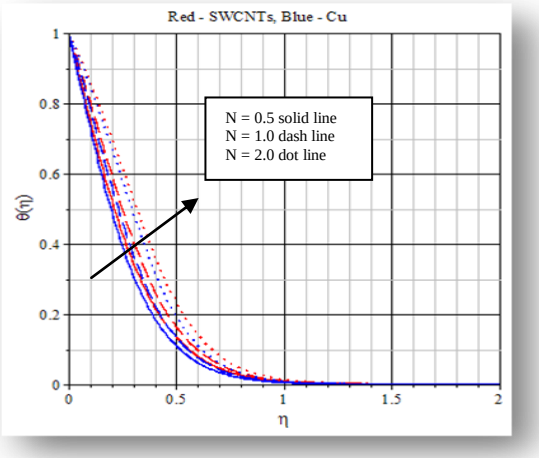

Fig.2 Effects of convective radiation on velocity and temperature profiles

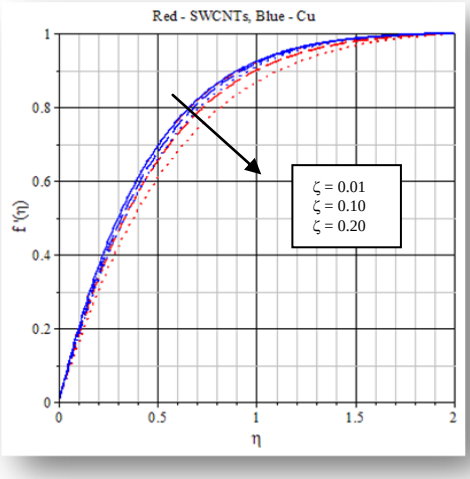

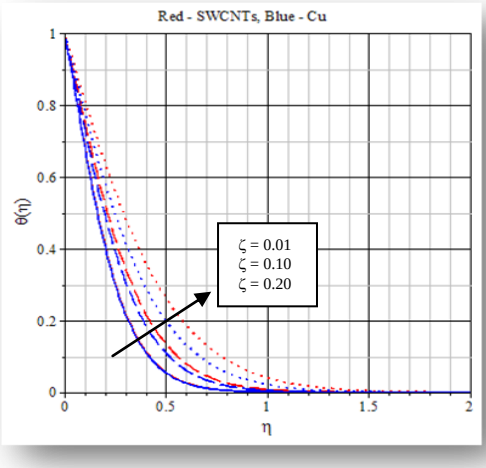

Fig.3 Effects of nanoparticle volume fraction on velocity and temperature profiles

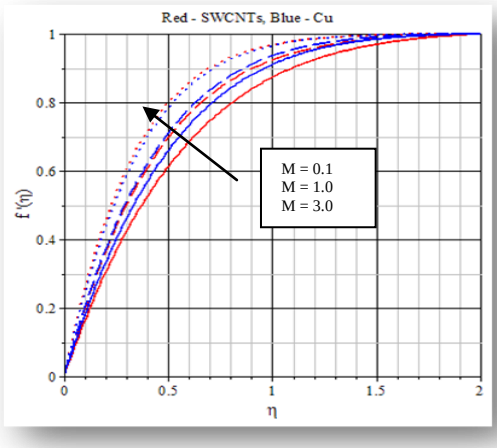

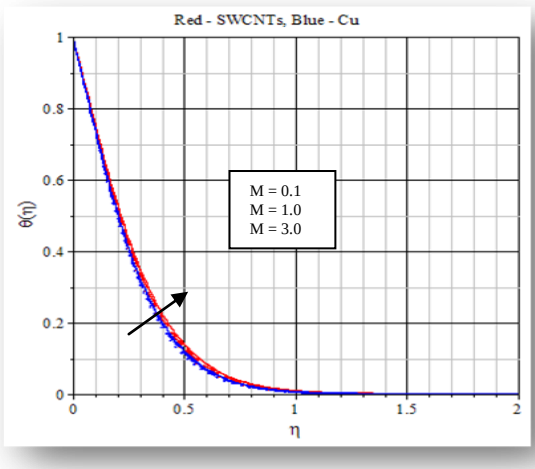

Fig.4 Effects of magnetic strength on velocity and temperature profiles

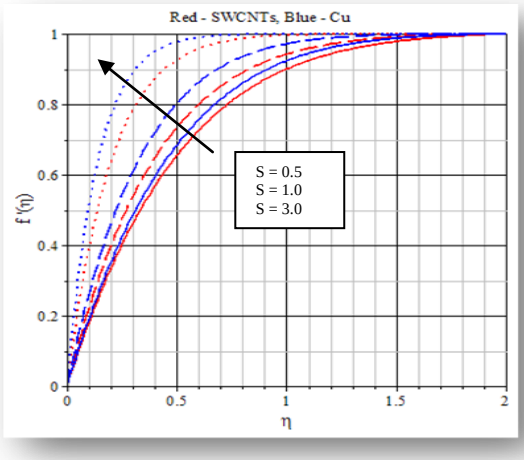

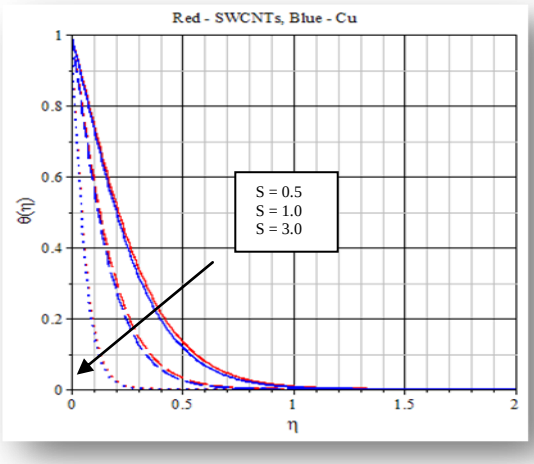

Fig.5 Effects of suction on velocity and temperature profiles

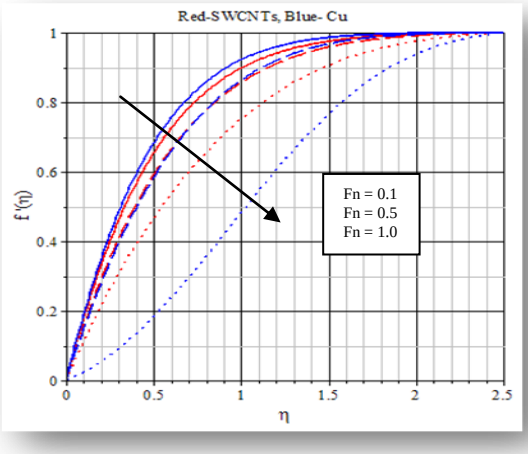

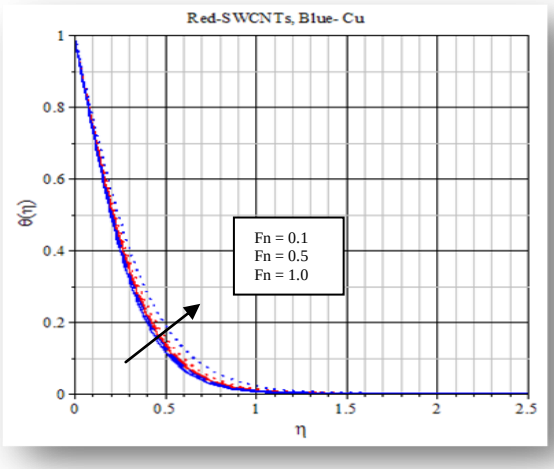

Fig.6 Effects of Forchheimer number on velocity and temperature profiles

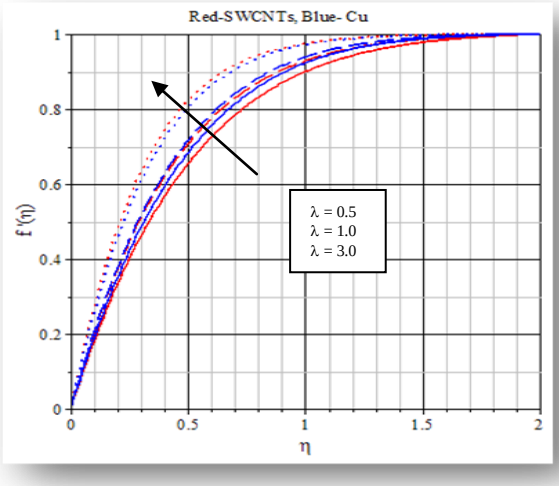

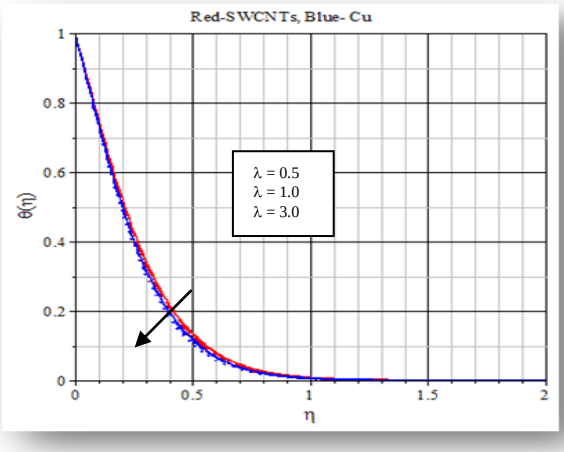

Fig. 7 Effects of porosity on velocity and temperature profiles

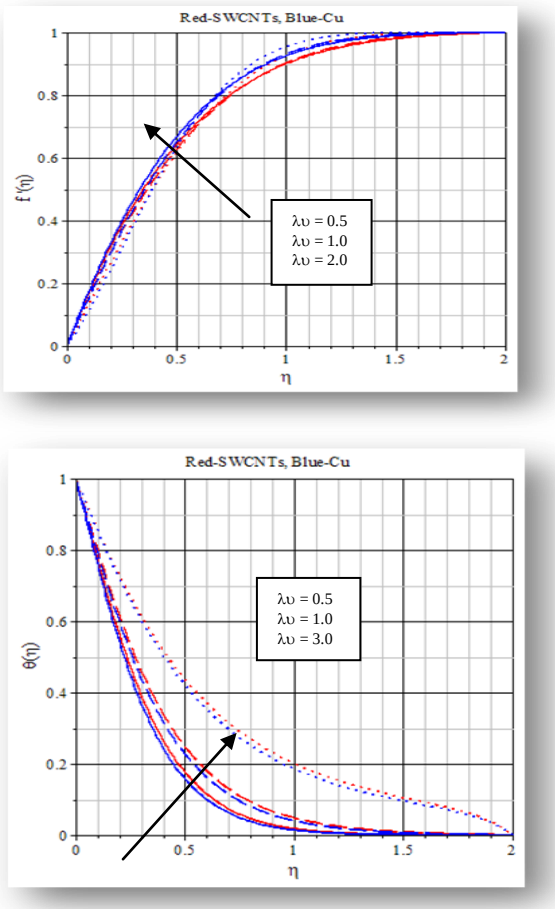

Fig.8 Effects of unsteady parameter on velocity and temperature profiles

Table 4 $f''(0)$ and $-\theta'(0)$ for different values of N with $S = 0.5, \Pr = 6.2, \lambda = 0.5, \gamma = 0.1, , Ec = 0.001, \delta = 0.5, \zeta = 0.1, M = 0.5$

N	$f''(0)$	$-\theta'(0)$
SWCNTs-water	0.1	1.814231058253637
		3.187780628843792
	1.0	1.839676499899816
		1.719771946768407
	2.0	1.863084855955898
		1.186912262517085
MWCNTs-water	0.1	1.839578186836152
		3.202680500438116
	1.0	1.866758333598846
		1.727841402032229
	2.0	1.891625555870828
		1.192524220187774

Figs. 1 presents typical profiles for velocity and temperature for different materials (Titania, Alumina, silver, copper and SWCNTs) in the presence of base fluid (water). Due to the uniform convective radiation, it is clearly shown that the velocity and the temperature of the nanofluid accelerate with the increase of the water based nanoparticles (Titania, Alumina, silver, copper and SWCNTs). It is observed that the temperature profiles for water based SWCNTs is higher than that of other nanoparticles, which implies that the SWCNTs show a unique combination of stiffness, strength, and tenacity compared to other fiber materials which usually lack one or more of these properties. Thermal and electrical conductivity of SWCNTs is also very high, and comparable to other conductive materials. Increase of thermal boundary layer field due to increase in thermal conductivity shows that the temperature field increases gradually as we replace Titania by Alumina, silver, copper and SWCNTs in the said sequence. Figs. 2 and 3 illustrate the characteristic velocity and temperature profiles for different values of the convective radiation N and the nanoparticle volume fraction in the presence of water based copper nanoparticles and SWCNTs. In both the cases, it is noticed that the temperature of the nanofluid increases with the increase of the convective radiation and nanoparticle volume fraction parameters. It is also observed that the temperature profiles for water based SWCNTs is stronger than that of copper nanofluid because of the combined effect of the thermal conductivity/density of the SWCNTs are higher/lower compared to the copper nanoparticles in the base fluid.

From the Figures 4 – 8, it is predicted that the water based SWCNTs plays a dominant role on velocity and temperature profiles compared to that of copper nanofluid with the increase of all the other parameters in this investigation. Enhancement in thermal conductivity of SWCNTs can lead to efficiency improvements, although small, via more effective fluid heat transfer. In convective heat transfer in nanofluid, the heat transfer depends not only on the thermal conductivity but also on other properties, such as the specific heat, density, and dynamic viscosity of the nanofluid (water based SWCNTs). Enhancement in thermal conductivity water based SWCNTs can lead to efficiency improvements, although small, via more effective fluid heat transfer. It is observed that the rate of heat transfer for SWCNTs, MWCNTs – water decreases with increase of thermal radiation,Table 4.

IV. CONCLUSIONS

Thermal boundary layer thickness of water based SWCNTs is stronger than that of the copper nanofluid as the strength of the convective radiation and the nanoparticle volume fraction increases because the carbon nanotubes experience an increase in temperature after being heated by the thermal radiation energy. It is observed that the temperature of water based SWCNTs is accelerated monotonically as compared to that of the copper nanofluid with an increase of convective radiation. It has been shown that mixing SWCNTs in a base fluid (water) have a dominant effect on the liquid thermophysical properties while the thermal conductivity of the water based SWCNTS is strongly dependent on nanoparticle volume fraction. SWCNTs in the presence of base fluid flow over a porous wedge plays a significant role on absorbs the incident thermal radiation and transmits it to the working fluid by convection. It is interesting to note that the thermal boundary layer thickness for SWCNTs – water is significantly stronger as compared to Cu-water to increase of thermal radiation, nanoparticle volume fraction and unsteady parameters because of the combined effects of thermal conductivity, and diffusivity of the nanoparticles and carbon nanotubes. The strength of rate of heat transfer for MWCNTs-water is significantly higher than that of SWCNTs –water in the presence of thermal radiation energy due to the joint effects of specific heat with thermal expansion and conductivity of MWCNTs. Water based SWCNTs have been proven to be excellent thermal and electrical conductors that can be used in thermal radiation energy technology because the thermal conductivity of SWCNTs is significantly higher than copper nanoparticles.

ACKNOWLEDGEMENT

The authors wish to express their cordial thanks to our beloved The Vice Chancellor and The Dean, FSTPi, UTHM, Malaysia for their encouragements and acknowledge the financial support received from FRGS 1208 /2013.

Nomenclature----------

B_0 : Magnetic flux density, $kg\ s^{-2}A^{-1}$

C_T : Temperature ratio, K

c_p : Specific heat at constant pressure, $J\ kg^{-1}K^{-1}$

Ec : Eckert number (-)

g : Acceleration due to gravity, ms^{-2}

Gr : Grashof number (-)

k_1 : Rate of chemical reaction, $mol\ m^{-1}s^{-1}$

k^*: Mass absorption coefficient, m^{-1}

K : Permeability of the porous medium, m^2

k_f :Thermal conductivity of base fluid, $kg\ m\ s^{-3}\ K^{-1}$

k_s :Thermal cond. Of nanoparticle, $kg\ m\ s^{-3}\ K^{-1}$

k_{nf} :Thermal cond. of the nanofluid, $kg\ m\ s^{-3}\ K^{-1}$

M : Magnetic parameter (-)

N : Thermal radiation parameter (-)

Pr : Prandtl number (-)

Re : Reynolds number (-)

q''_{rad} : Radiation flux of intensity, $kg\ m^{-1}\ s^{-3}\ K^{-1}$

Q_0 : Rate of source/sink, $kg\ m^{-2}$

t : Time, s

T : Temperature of the fluid, K

T_w : Temperature of the wall, K

T_∞ : Temperature of the fluid far away from the wall, K

x, y : Streamwise coordinates, m

u, v : Velocity components, $m\ s^{-1}$

$U(x)$: Flow velocity of the fluid at infinity, $m\ s^{-1}$

V_0 : Velocity of suction / injection, $m\ s^{-1}$

Greek symbols

α_{nf} : Thermal diffusivity of the nanofluid, $m^2\ s^{-1}$

β_f : Thermal expansion of the base fluid, K^{-1}

ρ_f : Density of the base fluid, $kg\ m^{-3}$

ρ_s : Density of the nanoparticle, $kg\ m^{-3}$

ρ_{nf} :Effective density of the nanofluid, $kg\ m^{-3}$

$(\rho c_p)_{nf}$:Heat capacitance of nanofluid, $J\ m^{-3}K^{-1}$

$(\rho\beta)_{nf}$:Volumetric expansion of nanofluid, K^{-1}

σ : Electric conductivity, $\Omega^{-1}m^{-1}$

σ_1 : Stefan – Boltzman constant, $kg\ s^{-3}\ K^{-4}$

μ_f : Dynamic viscosity of base fluid, $kg\ m^{-1}\ s^{-1}$

μ_{nf} : Dynamic viscosity of nanofluid, $kg\ m^{-1}\ s^{-1}$

ν_{nf} : Dynamic viscosity of the nanofluid, $m^2\ s^{-1}$

δ : Time-dependent length scale, s

λ : Porous parameter (-)

Ω : Resistance, $kg\ m^2 s^{-3} A^{-2}$

ζ : Nanoparticle volume fraction (-)

ψ : Dimensionless stream function (-)

η : Similarity variable (-)

f : Dimensionless stream function (-)

θ : Dimensionless stream function (-)

REFERENCES

[1]. Gaurav Lalwani, Andrea Trinward Kwaczala, Shruti Kanakia, Sunny C. Patel, Stefan Jude and Balaji Sitharaman, Fabrication and characterization of three-dimensional macroscopic all-carbon scaffolds, *Carbon*, 53(2013) 90–100.

[2]. D.A. Nield and A.V. Kuznetsov, The Cheng-Minkowycz problem for natural convective boundary-layer flow in a porous medium saturated by a nanofluid, *Int. J. Heat Mass Tran.*, 52(2009) 792–795.
[3]. A.V. Kuznetsov and D.A. Nield, Natural convective boundary-layer flow of a nanofluid past a vertical plate, *Int. J. Therm. Sci.*, 49(2010) 243–247.
[4]. W.A. Khan and I. Pop, Boundary-layer flow of a nanofluid past a stretching sheet, *Int. J. Heat Mass Tran.*, 53 (2010) 2477–2483.
[5]. Feng-Chao Wang and Ya-Pu Zhao, Slip boundary conditions based on molecular kinetic theory: The critical shear stress and the energy dissipation at the liquid–solid interface, *Soft Matter.*, 7(2011) 8628-8634.
[6]. M.M.J. Reacy, T.W. Ebbesen and J.M. Gibson, Exceptionally high Young's modulus observed for individual carbon nanotubes, *Nature*, 381 (1996) 678–680.
[7]. V. Zavalniuk and S. Marchenko, Theoretical analysis of telescopic oscillations in multi-walled carbon nanotubes, *Low Temperature Physics* 37(2011) 337-343.
[8]. Quanzi Yuan and Ya-Pu Zhao, Transport properties and induced voltage in the structure of water-filled single-walled boron-nitrogen nanotubes, *Biomicrofluidics*, 3 (2009) 022411.
[9]. Quanzi Yuan and Ya-Pu Zhao, Hydroelectric voltage generation based on water-filled single-walled carbon nanotubes, *Journal of the American Chemical Society*, 131 (2009) 6374–6376.
[10]. R. Kandasamy, I. Muhaimin and Rosmila, A.K., The performance evaluation of unsteady MHD non-Darcy nanofluid flow over a porous wedge due to renewable (solar) energy, *Renewable Energy*, 64(2014) 1-9.
[11]. E.M. Sparrow and R.D. Cess, Radiation heat transfer, *Hemisphere*, Washington, (1978).
[12]. M.A. Sattar, Local similarity transformation for the unsteady two-dimensional hydrodynamic boundary layer equations of a flow past a wedge, *Int. J. App. Math. & Mech.*, 7 (2011) 15-28.
[13]. K.G. Kafoussias and N.D. Nanousis, Magnetohydrodynamic laminar boundary layer flow over a wedge with suction or injection, *Canadian Journal of Physics*, 75(1997) 733-741.
[14]. R. Kandasamy, P. Loganathan and P. Puvi Arasu, Scaling group transformation for MHD boundary- layer flow of a nanofluid past a vertical stretching surface in the presence of suction / injection, *Nuclear Engg. and Design*, 241(2011) 2053-2059.
[15]. H. Schlichting, Boundary Layer Theory, *McGraw Hill Inc.*, New York (1979)

Appendix A

```
> restart;
> libname := Shootlib, libname :
> with(plots) :
Pr := 6.2; S := 0.5; Υ := 0.1; Ec := 0.001; a := 1; δ := 0.5; (B1) := 0.5; l := 0.1;
```

$Pr := 6.2$, $S := 0.5$, $\Upsilon := 0.1$, $Ec := 0.001$, $a := 1$,
$\delta := 0.5$, $B1 := 0.5$, $l := 0.1$

```
M := 0.5; Z := 0.1; Ξ := 0.5; n := 1; λ := 0.5; N := 0.5; p := 1.667; A := 0.333;
```

$M := 0.5$, $Z := 0.1$, $\Xi := 0.5$, $n := 1$, $\lambda := 0.5$,
$N := 0.5$, $p := 1.667$, $A := 0.333$

```
(CT) := 0.5; (ρs) := 2600; (ρf) := 997; (cps) := 425; (cpf) := 4179; (ks) := 6600; (kf)
    := 0.613; (βs) := 1.67E−5; (βf) := 21E−5;
```

$CT := 0.5$, $\rho s := 2600$, $\rho f := 997$, $cps := 425$,
$cpf := 4179$, $ks := 6600$, $kf := 0.613$,
$\beta s := 0.0000167$, $\beta f := 0.00021$

$$(Kfn) := (ks) + 2.(kf) - 2.\Upsilon.((kf) - (ks));$$

$Kfn := 7921.1034$

$$B := \left(1 - \Upsilon + \Upsilon.\frac{(\rho s)}{(\rho f)}\right); \quad B := 1.160782347$$

$$E := \left(1 - \Upsilon + \Upsilon.\frac{(\rho s).(cps)}{(\rho f).(cpf)}\right); \quad E := 0.9265212964$$

$$G := (1 - \Upsilon)^{2.5}; \quad G := 0.7684334714$$

$$\Omega := A.(180); \quad \Omega := 59.940$$

$$(Kf) := (ks) + 2.(kf) + 2.\Upsilon.((kf) - (ks));$$

$Kf := 5281.3486$

$$C := \frac{Kfn}{Kf}; \quad C := 1.499825897$$

$$FNS := \{f(\eta), u(\eta), v(\eta), \theta(\eta), w(\eta)\} :$$

$$ODE := \left\{ \mathrm{diff}(f(\eta),\eta) = u(\eta), \mathrm{diff}(u(\eta),\eta) = v(\eta), \mathrm{diff}(\theta(\eta),\eta) = w(\eta), diff(v(\eta),\eta) \right.$$

$$- \left(\frac{p.G}{B}\right).\left(\left(M + \frac{\lambda}{G}\right).\left(u(\eta)^2 - 1\right) - \left(\frac{E.a}{2}\right).\theta(\eta)\right) - B.G.\left((A - p.I).\left(u(\eta)^2 - 1\right)\right.$$

$$\left. - f(\eta).v(\eta) + \delta.(2 - \eta.v(\eta) - 2.u(\eta))\right) = 0, \mathrm{diff}(w(\eta),\eta)$$

$$+ \left(\frac{1}{1 + \left(\frac{4}{3}\right).\left(\frac{1}{C}\right).N.(0.1 + \theta(\eta))^3}\right).\left(\left(\frac{4}{C}\right).N.(0.1 + \theta(\eta))^2.w(\eta)^2 + \left(\frac{Pr}{G}\right).Ec\right.$$

$$\left. .v(\eta)^2 - Pr.\left(\frac{E}{C}\right).(p.n.u(\eta).\theta(\eta) - f(\eta).w(\eta) + \delta.\eta.w(\eta))\right) = 0\Big\};$$

$$ODE := \left\{ \frac{d}{d\eta} w(\eta) + \left(\frac{1}{1 + 0.4444960365\,(0.1 + \theta(\eta))^3}\right).\left(1.333488110\left(\left((0.1\right.\right.\right.\right.$$

$$\left.\left.\left.\left. + \theta(\eta))^2\right).\left(w(\eta)^2\right)\right) + 0.008068362755\,v(\eta)^2 - 6.384719870\,(u(\eta).\theta(\eta))\right.\right.$$

$$\left.\left. + 3.830065909\,(f(\eta).w(\eta)) - 1.915032954\,(\eta.w(\eta))\right) = 0, \frac{d}{d\eta} v(\eta)\right.$$

$$\left. - 1.418160955\,u(\eta)^2 + 0.5261769462 + 0.51123018\,62\,\theta(\eta) + 0.8919840084\,(f(\eta)\right.$$

$$\left. .v(\eta)) + 0.4459920042\,(\eta.v(\eta)) + 0.8919840084\,u(\eta) = 0, \frac{d}{d\eta} f(\eta) = u(\eta),\right.$$

$$\left. \frac{d}{d\eta}\theta(\eta) = w(\eta), \frac{d}{d\eta} u(\eta) = v(\eta)\right\}$$

$$(A1) := 1 + \frac{l}{(1 - \Upsilon)^{2.5}}; \quad A1 := 1.130134883$$

$$IC := \{f(0) = p.S, u(0) = 0, \theta(0) = 1, v(0) = \alpha, w(0) = \beta\};$$

$$IC := \{f(0) = 0.8335, \theta(0) = 1, u(0) = 0, v(0) = \alpha, w(0) = \beta\}$$

$$L := 2; \quad L := 2 \quad BC := \{u(\mathrm{L}) = 1, \theta(\mathrm{L}) = 0\};$$

$$BC := \{\theta(2) = 0, u(2) = 1\}. \quad infolevel[shoot] := 1 :$$

$$S := shoot(ODE, IC, BC, FNS, [\alpha = 1.8313159991271961, \beta = -2.291393377809066]) :$$

shoot: Step # 1,shoot: Parameter values : alpha = 1.8313159991271961 beta = -2.291393377809066
shoot: Step # 2,shoot: Parameter values : alpha = HFloat(1.8261209398868097) beta = HFloat(-2.289978355615486)